MATEC Web of Conferences **5**, 04041 (2013)
DOI: 10.1051/matecconf/20130504041
© Owned by the authors, published by EDP Sciences, 2013

Microstructural characterization of $CoMnFeO_4$ thin films deposited by radio-frequency sputtering

F. Oudrhiri-Hassani[1], L. Presmanes[2], A. Barnabe[2] and P. Tailhades[2]

[1] *ENSA de Safi, Route Sidi Bouzid, BP. 63, 46000 Safi, Maroc*
[2] *Institut Carnot Cirimat, 118, Route de Narbonne, 31062 Toulouse Cedex 09, France*

Abstract. $CoMnFeO_4$ thin films are stable materials useful to study the influence of radio-frequency sputtering experimental conditions, on the microstructure of oxide films. From various techniques of electronic microscopy, gas adsorption techniques and ellipsometry measurements, it was shown that such oxides films prepared with 0.5 Pa sputtering argon pressure and 5 cm target–substrate distance are very dense. On the other hand, the samples obtained under higher pressure and/or longer distance, are microporous. This porosity is mainly due to shadowing and energetic effects of sputtered particles. According to different characterization techniques, a simple model is proposed to describe the microstructure of the films studied.

1. INTRODUCTION

Recently, the spinel oxides have been successfully applied in several technological fields. In fact, their magnetic and electrical properties allow the use of these materials in information storage [1,2], in gas sensor [3,4] and in catalysts [5,6]. Spinels are often used in the form of thin films that are prepared by physical vapor deposition (PVD) techniques such as the radio-frequency sputtering. The latter holds dual interests like growing thin films with nanometric grains and also being perfectly compatible with micro-technologies. It is noteworthy, however, that thin films properties are highly depended on the microstructure [7–9]. The study presented here concerns the microstructural characterization of mixed cobalt manganese ferrite thin films prepared by RF sputtering. The choice of $CoMnFeO_4$ is due to its structural stability and low sensitivity to oxido-reduction phenomena. The impact of elaboration conditions on microstructure thin films will be discussed.

2. THIN FILMS PREPARATION

Mixed cobalt manganese ferrite thin films were deposited in an Alcatel A450 RF sputter system from a 10 cm in diameter $CoMnFeO_4$ target. The Alcatel A450 RF sputter machine was equipped with a radio-frequency-generator (13.56 MHz) device as well as a pumping system which allows reaching a residual pressure down to 10^{-5} Pa and a magnetron placed behind the target. The films were deposited on glass slides. A residual vacuum of 5.10^{-5} Pa was reached in the sputtering chamber before introducing the deposition gas (argon). In order to obtain various microstructures, different distances and argon pressures were used. The whole experimental conditions used to prepare 300 nm thin films, are summarized in Table 1.

The following step sheds light on evaluating the influence of these parameters on the films microstructure by using various characterization techniques. In the next part, the samples will be named "Pxdy", with x the value of argon pressure in Pascal, and y the sample target distance in millimeter.

Table 1. Experimental conditions carried out for samples preparation.

Argon Pressure (Pa)	0.5; 1; 1.5 and 2
Target-substrate distance (mm)	50; 65 and 80
Power density ($W.cm^{-2}$)	0.9
Film thickness (nm)	300
Substrate	Glass Slide

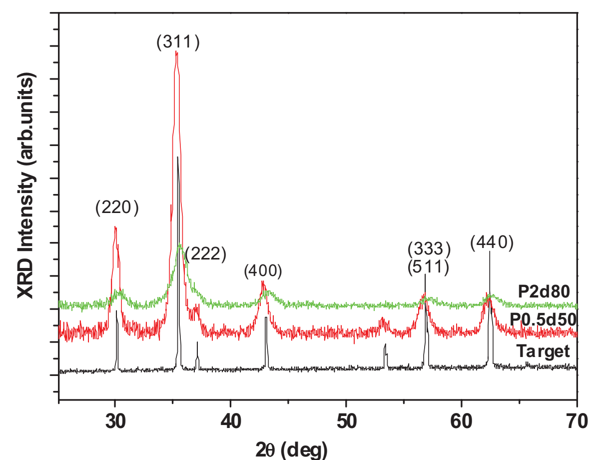

Figure 1. GIXRD patterns of $CoMnFeO_4$ thin films.

3. CHARACTERIZATIONS AND DISCUSSIONS

Structural characterizations of films were performed by grazing angle X-ray diffraction (GIRXD) on a Siemens D 5000 diffractometer. The X-ray diffraction patterns (figure 1) show the films are all made up of a single cubic spinel phase. The apparent crystallite size determined in θ–2θ mode from the full width at half maximum (FWHM) of (311) spinel peaks, applying pseudo distribution for the peak broadening, and using the Sherrer formula below, to deduce the apparent crystallite size:

$$\mathrm{FWHM} = \frac{K\lambda}{\Phi_{RX} \cos\theta} \tag{1}$$

This is an Open Access article distributed under the terms of the Creative Commons Attribution License 2.0, which permits unrestricted use, distribution, and reproduction in any medium, provided the original work is properly cited.

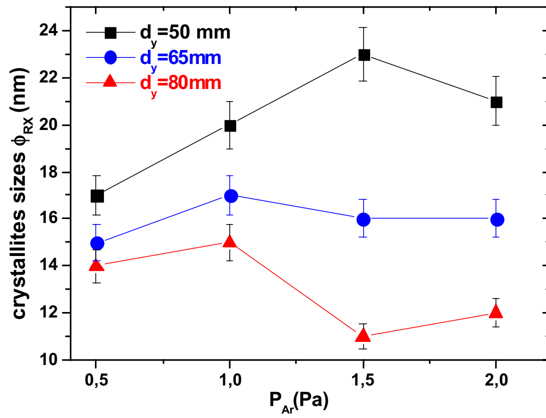

Figure 2. Variation of crystallites size according to the pressure of deposition for various distances target-substrate.

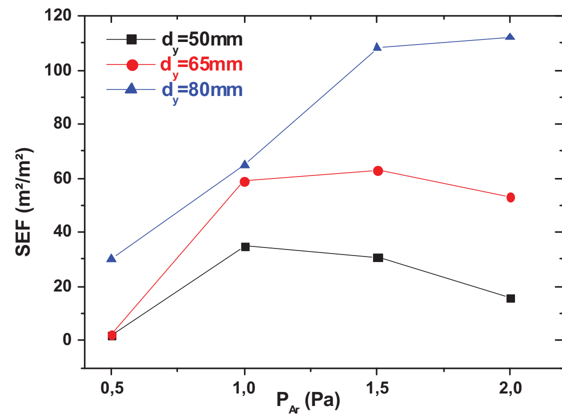

Figure 3. Variation of Surface Enhancement Factor according to argon pressure of deposition for various distances target-substrate.

where FWHM is size broadening corrected by the instrumental contribution and k is a constant, in this calculation k= 0.9, λ is the radiation wavelength (λ = 1.5406 Å for Cu $K_{\alpha 1}$), Φ_{RX} is apparent crystallite size and θ is Bragg angle.

The crystallite size $\Phi_{X\text{-ray}}$ varies as a function of conditions elaborations (Figure 2). Indeed, for a given argon pressure, $\Phi_{X\text{-ray}}$ seems to be decreased by increasing distance.

The crystallites size is related to the energy of various particles coming from the target to the surface of the layer in growth [7]. Therefore, taking into account this energy effect which is connected to the elaboration conditions, we thus expect significant microstructural changes in elaborate thin films. The images obtained by AFM and SEM microscopy techniques showed the same variation of the grains sizes as that calculated with x-rays diffraction technique [11]. The change of the microstructure was also observed. However, it was difficult to reach the porosity of films with these techniques of microscopy.

The use of B.E.T method to measure the specific area of thin films allows us to determine precisely the interganular porosity. The surface area measurements were done on freshly prepared samples with a Micromeritics ASAP 2010 operating with Krypton at liquid nitrogen temperature. Several (1.3 cm * 1.3 cm) square samples covered on each side by 300 nm thick oxide films were placed in the Micromeritics ASAP 2010 cell for each experiment. Prior to measurements, the samples were heated under vacuum at 300 °C for 16 h to clean their surfaces [9]. From krypton adsorption isotherms at 77 K the surface area can be measured for these samples. Because of the difficulty to measure the very low mass of the layers deposited, it was not possible to us to precisely determine the specific surface of films (generally expressed in m^2 /g in the case of the powders). We thus calculated the surface enhancement factor (SEF) defined by the surface area measured by krypton adsorption for a 1m*1m square part of a 300 nm thick film.

B.E.T. method proves to be a technique more effective than microscopy to give quantitative values making it possible to compare the intergranular porosity of various films. The curves SEF = f(P_{Ar}) (Figure 3) show that this factor is higher for the long distances target-substrate and high deposition pressure. This can be explained by the fact that the flow of particles extracted from plasma is concentrated on a small surface which increases the number of collisions occurring in the space between the target and the substrate and causes an increase of mean incident angle and thus, the appearance of shadowing effects leading to intergranular voids within the growing layer [9].

To supplement the information obtained from the analysis of the surface, we used the ellipsometry which makes it possible to connect the evolutions of optical indices n and k to the microstructure of the thin films. Ellipsometry was carried out with a spectroscopic ellipsometer in the whole visible spectral range of (350–800 nm). The fitting of ellipsometric data, was first modelled with the Tauc-Lorentz (TL) dispersion relations [12]. A sample stack structure glass/film/surface layer, was employed to extract the optical constants (n and k) of thin films. Most of the films studied are porous and the optical constants measured are related to the properties of both $CoMnFeO_4$ and voids [10]. Some samples however, are almost 100% dense, as demonstrated by surface area measurements and the high values of the refractive and absorptive indices (P0.5d50). The real optical constants of dense $CoMnFeO_4$ can then be obtained from these samples. To determine the porosity and to study the evolution of the films, a model is adopted considering a glass substrate of L1 = 1 mm thickness, covered by the oxide film made itself by two layers L2 and L3. The first one called (L2), in contact with the substrate, is completely dense, its thickness is L2 nanometers and its optical constants are those previously determined for dense $CoMnFeO_4$. The second layer (L3) of L3 nanometers, displays a porosity of p3 percent. The upper part (L4) of the film is made of a 50% porous layer having a thickness of L4 nanometers. Surface roughness and porous layers were modelled with the Bruggeman effective medium approximation (BEMA) [12], where the layers are constituted of a mixture of dense $CoMnFeO_4$ and void. We observed that n and k values changed for materials characterized, this variation is due to the

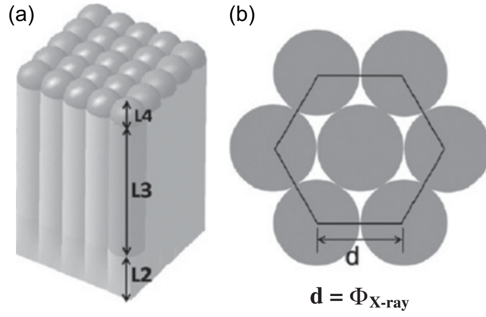

Figure 4. Microstructural model of the films (a) 3-D view (b) detail of the hexagonal arrangement of the rods [10].

material's porosity [10]. The highest optical constants were then acquired for the samples deposited under the conditions leading to the highest film density, i.e. P = 0.5 Pa.

4. MICROSTRUCTURAL MODEL

According to different characterization techniques, a simple model is proposed to describe the microstructure of the films studied (Figure 4).

This model was developed by using the crystallography principles and some geometry bases. The goal of the use of this model is to calculate volume porosity, SEF factor and the surface roughness (Ra), then, to compare these parameters with those which were given in experiments for all films deposited under various conditions of deposit. According to Figure 4, the films are made of three layers. The first one (L2), located at the interface with the substrate, is 100% dense. The second layer (L3), covering the previous one, is made of cylindrical rods arranged according a hexagonal lattice. Its porosity is due to the lattice interstices. Hemispheric domes covering each rod make up the third layer (L4), which displays a roughness related to the shape and the hexagonal arrangement of the domes. The microstructure of the (L3) and (L4) layers then looks like the microstructures described by Thornton [13] when the deposition temperature is low. The specific surface area (SEF), the porosity (p) and the roughness (Ra), calculated from the model, are presented as follow:

$$\mathrm{SEF} = \frac{(4\mathrm{L}_3 + \mathrm{d})\pi + 2 \cdot \mathrm{d} \cdot \sqrt{3}}{2 \cdot \mathrm{d} \cdot \sqrt{3}} \tag{2}$$

$$\mathrm{p} = \frac{6\sqrt{3}\mathrm{L}_3 + 3\sqrt{3}\mathrm{d} - \pi \cdot (3\mathrm{L}_3 + \mathrm{d})}{3\sqrt{3}(2\mathrm{L}_2 + 2\mathrm{L}_3 + \mathrm{d})} \tag{3}$$

$$\mathrm{R}_\mathrm{a} \approx 0.123\mathrm{d}. \tag{4}$$

The calculation of these parameters is previously detailed in other publication [10]. The values obtained are in good agreement with the experimental results.

5. CONCLUSION

The use of various techniques such as electronic microscopy, measurements of surface B.E.T. and ellipsometry has clearly shown the passage from a dense microstructure to a porous microstructure by changing the elaboration conditions (pressure of argon and distance target-substrate). For instance, with low pressure and short distance target-substrate, we obtained dense films, while the use of high pressures and long distances target-substrate, made it possible to increase the intergranular porosity of films.

References

[1] Corine Despax, Philippe Tailhades, Carole Baubet, Carole Villette, Abel Rousset; Thin Solid Films **293** (1997).
[2] Yan Wang, D.F. Li, J.Y. Dai, Journal of Crystal Growth **313** (2010)
[3] G. Neri, A. Bonavita, S. Galvagno, P. Siciliano, S. Capone, Sensors and Actuators B **82** (2002).
[4] Hiroyuki Yamaura, Teruyuki Jinkawa, Jun Tamaki, Koji Moriya b, Norio Miura, Noboru Yamazoe, Sensors and Actuators B **35-36** (1996).
[5] Dae-Chul Kim and Son-Ki Ihm, Environ. Sci. Technol. **35** 1 (2001).
[6] Kajornsak Faungnawakij, Naohiro Shimoda, Tetsuya Fukunaga, Ryuji Kikuchi, Koichi Eguchi, Applied Catalysis A **341** (2008).
[7] Stéphanie Capdeville, Pierre Alphonse, Corine Bonningue, Lionel Presmanes, and Philippe Tailhades, J. Appl. Phys. **96** (2004).
[8] David L. Young, Helio Moutinho, Yanfa Yan, and Timothy J. Coutts, J. Appl. Phys. **92** (2002)
[9] Izabela Sandu, Lionel Presmanes, Pierre Alphonse, Philippe Tailhades, Thin Solid Films **495** (2006).
[10] Fahd Oudrhiri-Hassani, Lionel Presmanes, Antoine Barnabe, Philippe Tailhades, Applied Surface Science **254** (2008).
[11] G.E. Jellison, F.A. Modine, Appl. Phys. Lett. **69** (1996).
[12] D.A.G. Bruggeman, Ann. Phys. Leipzig **24** (1935).
[13] J.A. Thornton, J. Vac. Sci. Technol. **11** (1974).